forum acusticum 2026
8-12 September · Graz, Austria

EFFICIENT CAD-BASED BROADBAND ACOUSTIC ANALYSIS AND SHAPE DESIGN USING REDUCED-ORDER IGABEM MODELS

Philip Le[1,3], Dionysios Panagiotopoulos[2,3], Emin Oguz Inci[4], Elke Deckers[1,3]

[1] *KU Leuven, Department of Mechanical Engineering, Campus Diepenbeek, Diepenbeek, Belgium*
[2] *KU Leuven, Department of Mechanical Engineering, Campus De Nayer, St.-Katelijne Waver, Belgium*
[3] *FlandersMake @KU Leuven*
[4] *Forcebit BV, Kessel-Lo, Belgium*

This paper is a revised version of the authors' submitted manuscript that was peer-reviewed by at least two anonymous reviewers.

Abstract

Broadband acoustic analysis and design of realistic computer-aided design (CAD) geometries are challenging due to the non-affine frequency dependence of the Boundary element method. When combined with isogeometric analysis (IGABEM), exact CAD geometry representation, high accuracy, and relaxed mesh requirements are offered. However, the use of spline-based basis functions increases the computational cost per degree of freedom, making analyses and iterative design loops computationally demanding. In that context, this work presents an efficient IGABEM-based framework that enables broadband acoustic shape exploration by combining IGABEM with a non-intrusive two-step model order reduction (MOR) strategy [1]. The frequency-dependent boundary element system is approximated and reduced using Krylov-subspace recycling MOR and reduced basis method, allowing fast evaluation of acoustic responses over wide frequency ranges. Shape variations are performed directly at the CAD level by modifying NURBS control points supported by a topological ring-based smoothing strategy to ensure smooth and robust geometry updates. The methodology is demonstrated on an academic example, a multi-patch non-conforming flat plate subjected to broadband acoustic excitation. The result shows that geometry smoothing leads to more natural shape variations, while the reduced-order model makes acoustic evaluations computationally feasible.

Keywords: *model order reduction, boundary element method, isogeometric analysis, shape optimization*

Corresponding author: *philip.le@kuleuven.be.*

1. Introduction

The accurate prediction of broadband acoustic behavior is essential in many engineering applications, including automotive noise radiation and exterior sound propagation. The Boundary element method (BEM) [2] is particularly attractive for such problems, as it reduces the problem dimensionality by one and inherently satisfies the radiation condition at infinity. Since BEM formulations discretize the entire geometry as a boundary surface, the accuracy of the acoustic solution is strongly influenced by the geometric representation of the domain. In traditional boundary element discretizations, low-order basis functions are commonly employed, leading to piece-wise geometry approximations that can introduce geometric errors and affect solution accuracy.

By following the isogeometric analysis (IGA) paradigm, spline-based basis functions such as Non-Uniform Rational B-splines (NURBS) are employed for both geometry representation and computation, thereby preserving the exact CAD boundary description within the analysis [3]. The combination of IGA and BEM (IGABEM) is popular in computational acoustics [4], [5] as it offers improved accuracy per degree of freedom (DOF) due to the high continuity of spline-based basis functions. This furthermore mitigates geometric approximation and pollution errors [6] compared to traditional boundary element discretizations. Nevertheless, the extended support over multiple knot spans of spline-based basis functions increases the computational cost per DOF, and the non-affine frequency dependence of the BEM operator prevents the efficient reuse of system matrices across frequency sweeps. As a result, broadband IGABEM analyses remain computationally expensive.

To reduce computational complexity, model order reduction (MOR) methods have been widely studied in context of frequency-domain acoustic BEM. Krylov

subspace-based MOR approaches in combination with either a Taylor series expansion [7] or Chebyshev polynomial approximation [8] have been applied as they offer a fast and high quality construction of the projection basis. However, Krylov-subspace MOR methods only lead to moderate reductions and are dependent on the spectral properties of the underlying system matrix. In IGABEM formulations, the extended support of spline-based basis functions leads to poor condition numbers which can reduce the efficiency of Krylov-subspace based MOR techniques. To address this, a second reduction step has been introduced for acoustic BEM systems, resulting in a highly efficient approach [1].
In this work, which presents a short version of the framework introduced in [9], a CAD-based IGABEM framework is presented in which a non-intrusive MOR strategy is employed to enable efficient broadband acoustic analysis and shape design on realistic CAD geometries. The MOR method employs an adaptive Krylov-subspace recycling MOR with Chebyshev polynomial approximation and reduced basis method (RBM). Shape variations are performed directly at the CAD level by modifying the NURBS control points, avoiding remeshing and geometry approximation. A topological ring-based smoothing strategy is introduced to ensure smooth and physically meaningful geometry updates. The approach is demonstrated on an academic test case consisting of a non-conforming flat plate excited by a unit-amplitude monopole source, where a particle swarm optimizer is used to illustrate how reduced-order models enable practical broadband shape design studies.

2. Isogeometric boundary element method

In this section the acoustic indirect Galerkin BEM with IGA is briefly introduced. For a more detailed derivation of the indirect BEM, the interested reader is referred to [10].

2.1. The indirect boundary element method with a Galerkin approach

By employing the fundamental solution, the Green's function $G : \mathbb{R}^3 \times \mathbb{R}^3 \to \mathbb{C}$, of the Helmholtz operator and considering both sides of the boundary surface Γ, the acoustic pressure can be represented in terms of potentials on the boundary. This leads to the indirect boundary integral equation

$$p_a(\mathbf{r}) = \int_\Gamma \left[\mu(\mathbf{r}_f) \frac{\partial G(\mathbf{r}, \mathbf{r}_f)}{\partial \mathbf{n}} - G(\mathbf{r}, \mathbf{r}_f)\sigma(\mathbf{r}_f) \right] d\Gamma, \quad \mathbf{r} \in \Omega \setminus \Gamma, \tag{1}$$

where $\mathbf{n}$ is the outward normal vector, the single layer potential $\sigma(\mathbf{r}_f)$ is the difference of the normal pressure gradient between two sides of the boundary Γ, and the double layer potential $\mu(\mathbf{r}_f)$ is defined as the difference in normal pressures between two sides of the boundary Γ.

2.2. Isogeometric Galerkin Discretization

To obtain a symmetric system model, a Galerkin approach is adopted. The unknowns, the single and double layer potential, are approximated using the same basis functions employed for the geometric representation, following the isogeometric concept.
The CAD boundary surface is represented by a NURBS surface patch

$$S(\xi, \eta) = \sum_{i=1}^{n} \sum_{j=1}^{m} R_{i,j}^{p,q}(\xi, \eta)\mathbf{P}_{i,j}, \tag{2}$$

where $R_{i,j}^{p,q}(\xi, \eta)$ is the bivariate NURBS basis function and $\mathbf{P}_{i,j} \in \mathbb{R}^d$ denote the control point. $R_{i,j}^{p,q}(\xi, \eta)$ can be written in terms of the tensor product of 2D B-spline basis functions $N_i^p(\xi)$ and $M_j^q(\eta)$ with polynomial orders, p, q and the knot vectors, $\Xi^1 = [\xi_1, ..., \xi_{n+p+1}]$ and $\Xi^2 = [\eta_1, ..., \eta_{m+q+1}]$ with $(\xi, \eta) \in [0,1] \times [0,1]$, respectively. The NURBS basis functions $R_i^p(\xi)$ of polynomial order p are defined as

$$R_i^p(\xi) = \frac{N_i^p(\xi)w_i}{\sum_{i=1}^{n} N_i^p(\xi)w_i} \quad \text{with } i = 1, ..., n, \tag{3}$$

where $N_i^p(\xi)$ is the i^{th} B-spline basis function of p^{th} degree and w_i are the weights. By following a Galerkin formulation, a global system of equations can be assembled in form of

$$\mathbf{A}(\omega)\mathbf{x}(\omega) = \mathbf{b}(\omega), \qquad \omega \in \Psi, \tag{4}$$

where $\mathbf{A} : \Psi \to \mathbb{C}^{N \times N}$ is the symmetric system matrix, $\omega := 2\pi f$ with f representing the frequency and $\omega \in \Psi := [\omega_{\min}, \omega_{\max}]$ and $\mathbf{b}, \mathbf{x} : \Psi \to \mathbb{C}^N$ are the force vector resulting from the imposed boundary conditions. Eq. (4) is solved for $\mathbf{x}$ which yields the discretized single layer potential and double layer potential.

3. Two-step model order reduction

To enable efficient broadband analyses, the two-step model reduction method is introduced. The method employs Chebyshev polynomials to decouple the frequency dependence of the non-affine IGABEM system. This enables a Galerkin projection onto a reduced subspace, where an adaptive Krylov subspace recycling method [8] is employed to construct an initial reduction basis. As Krylov-subspace based MOR methods only offer moderate reductions, a second reduction using RBM is employed on the affine reduced IGABEM system, to further reduce computational cost.

3.1. IGABEM approximation with Chebyshev polynomials

To obtain an affine representation, Chebyshev polynomials are leveraged to approximate the frequency-dependent IGABEM system matrix over the interval Ψ. The system matrix can be displayed as

$$\left(\sum_{i=0}^{\mathscr{M}}{}' c_i(\omega)\mathbf{T}_i\right)\mathbf{x}(\omega) = \sum_{i=0}^{\mathscr{M}}{}' c_i(\omega)\mathbf{q}_i, \tag{5}$$

where $c_i(\omega)$, with $i = 0, ...\mathscr{M}$, represent the Chebyshev polynomials of the first kind. The prime indicates that the first term is halved. By considering the maximum dimension of the model and Ψ, the truncation order of the Chebyshev polynomial approximation can be predetermined as suggested in [11]. The frequency independent parameters of the polynomial $\mathbf{T}_i \in \mathbb{C}^{N\times N}$ and $\mathbf{q}_i \in \mathbb{C}^N$ are defined as follows

$$\begin{aligned} \mathbf{T}_i &= \frac{2}{\mathscr{M}+1}\sum_{k=0}^{\mathscr{M}} \mathbf{A}(\omega_k)\, c_i(\omega_k), \\ \mathbf{q}_i &= \frac{2}{\mathscr{M}+1}\sum_{k=0}^{\mathscr{M}} \mathbf{b}(\omega_k)\, c_i(\omega_k) \end{aligned} \tag{6}$$

where the positions of the Chebyshev nodes ω_k correspond to the n zeros of the polynomials in the interval $[-1, 1]$ and are obtained by

$$\omega_k = \cos(\frac{\pi(k+\frac{1}{2})}{\mathscr{M}+1}). \tag{7}$$

To compute the true position of the Chebyshev nodes for $\omega \in \Psi$, a linear mapping of $\Psi \rightarrow (-1, 1)$ is needed. Eq. (6) expresses the system as a linear combination of frequency-independent matrices weighted by Chebyshev polynomials, enabling efficient assembly. The affine representation, however, increases memory requirements due to storage of the precomputed dense matrices.

3.2. Galerkin model order reduction in IGA-BEM

To reduce memory and computational cost, a Galerkin projection is applied to the Chebyshev-approximated IGABEM system. The system is approximated in a reduced subspace spanned by the columns of $\mathbf{W} \in \mathbb{C}^{N\times l}$,

$$\mathbf{x}(\omega) \approx \hat{\mathbf{x}}(\omega) = \mathbf{W}\tilde{\mathbf{x}}(\omega). \tag{8}$$

Enforcing the Galerkin orthogonality condition yields the reduced system

$$\mathbf{W}^{\mathrm{H}}\mathbf{A}(\omega)\mathbf{W}\tilde{\mathbf{x}}(\omega) = \mathbf{W}^{\mathrm{H}}\mathbf{b}(\omega), \tag{9}$$

Combining this projection with the Chebyshev approximation results in the following formulation

$$(\sum_{i=0}^{\mathscr{M}}{}' c_i(\omega)\mathbf{W}^{\mathrm{H}}\mathbf{T}_i\mathbf{W})\tilde{\mathbf{x}}(\omega) = \sum_{i=0}^{\mathscr{M}}{}' c_i(\omega)\mathbf{W}^{\mathrm{H}}\mathbf{q}_i, \tag{10}$$

yielding a compact form of

$$(\sum_{i=0}^{\mathscr{M}}{}' c_i(\omega)\mathbf{T}_{i,\mathrm{red}_{\mathrm{AKR}}})\tilde{\mathbf{x}}(\omega) = \sum_{i=0}^{\mathscr{M}}{}' c_i(\omega)\mathbf{q}_{i,\mathrm{red}_{\mathrm{AKR}}}. \tag{11}$$

Projecting $\mathbf{T}_i$ and $\mathbf{q}_i$ right after its assembly, reduces the size of the coefficient matrices and consequently, ensures that the memory requirements remain within the limits of the IGABEM.

3.3. Automatic Krylov subspaces recycling

To preserve the high-fidelity behavior of the full-order model (FOM), an automatic Krylov subspace recycling (AKR) algorithm [8] is employed. Instead of assembling and solving $\forall\omega \in \Phi$, where Φ is a discrete set with $|\Phi| = N_{\mathrm{tot}}$ and N_{tot} is the number of systems to be resolved, the AKR algorithm recycles Krylov subspaces only for $\omega \in \Omega_M$, where $\Omega_M := [\omega_1, ..., \omega_L]$ is a discrete ordered set with $\Omega_M \subset \Psi$ and $|\Omega_M| \ll |\Phi|$. For each sampled ω_j, a Krylov subspace is constructed by the Arnoldi algorithm [12]

$$\begin{aligned} \mathcal{K}_{m(\omega_j)}(\mathbf{A}(\omega_j), \mathbf{r}_0(\omega_j)) := \mathrm{span}\Big\{&\mathbf{r}_0(\omega_j), \mathbf{A}(\omega_j)\mathbf{r}_0(\omega_j), \\ &\ldots,\quad \mathbf{A}^{m-2}(\omega_j)\mathbf{r}_0(\omega_j), \mathbf{A}^{m-1}(\omega_j)\mathbf{r}_0(\omega_j)\Big\} \\ &= \mathrm{span}\{\mathbf{V}_{\omega_j}\}, \end{aligned} \tag{12}$$

where $m(\omega_j)$ with $j = 1, ..., L$ denotes the dimension of the respective Krylov subspaces for each $\omega_i \in \Omega_M$ and $L := |\Omega_M|$, $\mathbf{r}_0 = \mathbf{b} - \mathbf{A}\mathbf{x}_0$ with $\mathbf{x}_0 : \Psi \rightarrow \mathbb{C}^N$ an initial guess of the solution denotes the initial residual. The residual norm $|\mathbf{r}(\omega)| \leq r_{\mathrm{thresh}}, \quad \forall\omega \in \Psi$ serves as an error indicator to adaptively determine both the subspace dimensions $m(\omega_j)$ Ω_M through the AKR algorithm. A modified Gram-Schmidt orthogonalization is performed to prevent numerical instabilities [13]. A global reduction basis $\mathbf{W}$ spans the Krylov subspaces

$$\mathrm{span}\{\mathbf{W}\} = \bigcup_{j=1}^{L} \mathcal{K}_m(\omega_j). \tag{13}$$

Further algorithmic details are given in [8].

3.4. Second reduction step via Reduced basis method

Although the AKR algorithm provides an initial reduction, the achievable compression remains moderate for ill-conditioned or highly resonant systems, and storage of the reduced affine coefficient matrices may still become prohibitive [7]. By exploiting the reduced affine representation of the IGABEM system, a second reduction step based on the RBM [14] is introduced to further reduce computational costs. The RBM constructs an additional projection basis $\mathbf{V}_{\mathrm{RBM}}$ by sampling frequency snapshots at $\omega_{\bar{\kappa}+1} \in \Omega_{\mathrm{RBM}} \subset \Psi$, where Ω_{RBM} is a discrete ordered set with $|\Omega_{\mathrm{RBM}}| \ll |\Phi|$, using a greedy strategy. A residual based error estimator is used and is defined as

$$\begin{aligned} \mathbf{r}_{\mathrm{RBM},\bar{\kappa}}(\omega) := \mathbf{A}_{\mathrm{red}}(\omega)\bar{\mathbf{V}}_{\bar{\kappa}}\tilde{\mathbf{x}}_{2\mathrm{Step}}(\omega) - \mathbf{b}_{\mathrm{red}}(\omega), \\ \forall\,\omega \in \Phi \subset \Psi. \end{aligned} \tag{14}$$

where $\bar{\mathbf{V}}_{\bar{\kappa}}$ denotes the reduced basis from concatenating the $\bar{\kappa}$ snapshots. In each iteration, the snapshot corresponding to the maximum residual norm is selected and appended to the basis. The enrichment continues until $r_{\mathrm{RBM}} := ||\mathbf{r}_{\mathrm{RBM},\bar{\kappa}}(\omega)|| \leq r_{\mathrm{tol}}, \forall\omega \in \Phi$. The final RBM basis is then defined as $\mathbf{V}_{\mathrm{RBM}} := \bar{\mathbf{V}}_{\bar{\kappa}}$. Applying this second projection to the affine reduced system yields

$$\left(\sum_{i=0}^{\mathscr{M}} c_i(\omega)\,\mathbf{T}_{i,2\mathrm{Step}}\right)\tilde{\mathbf{x}}_{2\mathrm{Step}}(\omega) = \sum_{i=0}^{\mathscr{M}} c_i(\omega)\,\mathbf{q}_{i,2\mathrm{Step}} \tag{15}$$

The two-step MOR method produces a computationally efficient ROM, which allows rapid system evaluations across a broadband frequency range Ψ. This enables practical design iterations, where CAD-level geometry updates and multiple frequency-domain simulations are required.

4. Shape optimization

Geometric shape modifications are performed directly at the CAD level by modifying selected NURBS control points. The optimization problem over the frequency range $\Psi = [\omega_{\min}, \omega_{\max}]$ is formulated as

$$\min_{\mathbf{d}} J(\mathbf{d}) = \int_{\omega_{\min}}^{\omega_{\max}} \sum_{m=1}^{N_m} |p_a^m(\omega, \mathbf{d})|^2\, d\omega, \tag{16}$$

subject to bound constraints $\mathbf{d}^{\min} \leq \mathbf{d} \leq \mathbf{d}^{\max}$, where $\mathbf{d} \in \mathbb{R}^{n_{\mathrm{DV}}}$ denotes the vector of design variables, p_a^m is the acoustic pressure at microphone m, and N_m is the number of microphones.

4.1. Topological ring-based smoothing

To ensure smooth and physically meaningful deformations, each design variable induces displacements $\Delta\mathbf{P}_{i,j}^{\ell}$ on neighboring control points within the same patch. The resulting control point update is obtained by a normalized superposition

$$\Delta\mathbf{P}_{i,j} = \frac{\sum_{\ell} w_{i,j}^{\ell}\Delta\mathbf{P}_{i,j}^{\ell}}{\sum_{\ell} w_{i,j}^{\ell}}, \tag{17}$$

where $w_{i,j}^{\ell}$ are the weights of the decay function based on the ring distance. Thus, control points closer to the design variable undergo larger displacements, while points at a greater ring distance are attenuated. This strategy ensures smooth and realistic shape variations during the optimization.

4.2. Particle swarm optimization

Due to the ill-conditioned IGABEM system, a gradient-free particle swarm optimization (PSO) algorithm is employed. Each particle i represents a candidate design vector $\mathbf{d}_i$. At iteration k, velocities and positions are updated as

$$\mathbf{v}_i^{k+1} = w\,\mathbf{v}_i^k + c_1 r_1(\mathbf{p}_i - \mathbf{d}_i^k) + c_2 r_2(\mathbf{g} - \mathbf{d}_i^k), \tag{18}$$

$$\mathbf{d}_i^{k+1} = \mathbf{d}_i^k + \mathbf{v}_i^{k+1}, \tag{19}$$

where $\mathbf{p}_i$ and $\mathbf{g}$ denote the personal and global best positions, w is the inertia weight, c_1, c_2 are acceleration coefficients, and $r_1, r_2 \sim \mathcal{U}(0,1)$ are random scalars. For each particle, the updated geometry is evaluated using the reduced-order IGABEM solver, rendering broadband optimization computationally feasible.

5. Results

For the assessment of the proposed IGABEM MOR framework, a benchmark acoustic test case consisting of a multi-patch flat plate is considered (Fig. 1a). The 1×1 m plate is discretized into 4 non-conforming NURBS patches of degree $p = q = 2$, resulting in 492 DOFs, which are sufficient to accurately resolve acoustic responses up to 1000 Hz. A unit amplitude monopole source is located at $(0.25, 0.25, 0.5)$ m above the plate, radiating into the unbounded acoustic domain (Fig. 1b). The acoustic pressure is evaluated at nine microphone points forming a 3×3 grid with $x, y \in \{0.65, 0.75, 0.85\}$ m, located in a plane at $z = -0.5$ m. The frequency range is defined as $\Psi := [1, 1000]$ Hz with 1 Hz resolution which leads to 1000 dense linear systems in the FOM. For this problem a truncation order of $\mathscr{M} := 25$ is selected.

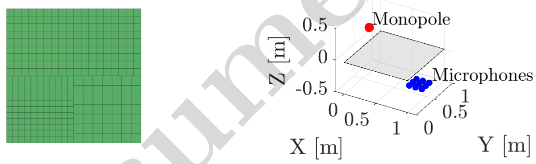

(a) Flat plate discretization **(b)** Flat plate subjected to a monopole source

Figure 1: Flat plate discretization and problem setup.

5.1. Performance of the two-step MOR for IGABEM systems

To assess the accuracy of the reduced-order model (ROM), the normalized residual is used as criterion and is defined as

$$||\mathbf{r}_{\mathrm{norm}}(\omega)|| := \frac{||\mathbf{A}(\omega)(\mathbf{W}(\mathbf{V}_{\mathrm{RBM}}\tilde{\mathbf{x}}_{2\mathrm{Step}}(\omega))) - \mathbf{b}(\omega)||}{||\mathbf{b}(\omega)||}. \tag{20}$$

The residual thresholds are set to $r_{\mathrm{thresh}} = 10^{-2}$ and $r_{\mathrm{tol}} = 10^{-3}$. The sound pressure level (SPL) from the FOM and ROM in Fig. 2 shows no differences over the entire frequency range Ψ, implying that the considered residual thresholds are sufficient. By inspecting the normalized residual, it can be observed that the predefined tolerance of 10^{-2} is satisfied over the majority of Ψ. Slight violations occur near 250 Hz, which can be attributed to the bisection sampling strategy employed by the AKR algorithm (Fig. 3). The corresponding sampling patterns for the construction of Ω_M, $\mathbf{W}$, $\mathbf{V}_{\mathrm{RBM}}$ are displayed in Fig. 4. For the flat plate, the AKR algorithm necessitates 9 full system assemblies and 5 partial solutions to construct $\mathbf{W}$. Additionally, 25 full system assemblies are employed to construct the Chebyshev coefficient matrices. The resulting ROM contains merely 21 DOFs.

5.2. Computational cost of the two-step MOR

The computational cost of the flat plate example is summarized in Table 1-2. For the two-step MOR, the highest computational cost stems from the construc-

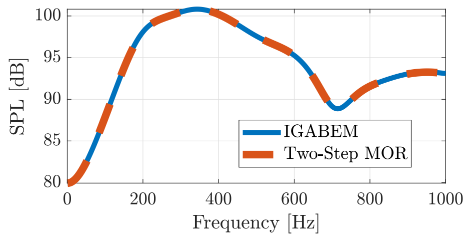

Figure 2: Initial response at $(0.65, 0.65, -0.5)$ m; flat plate subjected to a unit-amplitude monopole source.

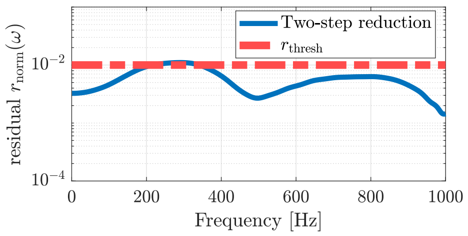

Figure 3: Normalized residual employing two-step MOR

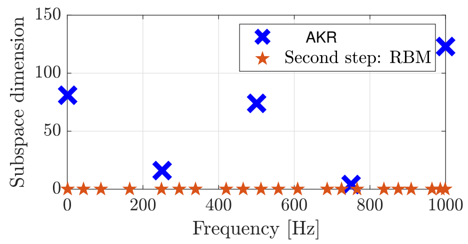

Figure 4: Sampling pattern of each step employing two-step MOR

tion of the Chebyshev coefficient matrix $\mathbf{T}_i$, followed by the construction of the initial reduction basis $\mathbf{W}$. The construction of $\mathbf{V}_{\mathrm{RBM}}$ is negligible as it only requires the selection of frequency snapshots using a greedy scheme of the reduced affine system. Once the off-line stage is completed, the on-line assembly and solution of the ROM yields speed-up factors of 10^3 and 10^2 compared to the FOM, respectively.

5.3. Broadband shape optimization

The IGABEM MOR framework enables efficient frequency sweep analyses, which can be also used in design optimization. For the broadband shape optimization of the flat plate, 6 control points are selected as design variables with displacement bounds of ± 0.1 m (Fig. 5a). A PSO algorithm with 12 particles and a maximum of 100 iterations is employed. The PSO is configured with an inertia weight decreasing linearly from $w_{\max} = 0.9$ to $w_{\min} = 0.4$ over the iterations, cognitive and social acceleration coefficients $c_1 = c_2 = 1.5$, and a maximum particle velocity $v_{\max} = 0.1 \times (\mathbf{d}^{\max} - \mathbf{d}^{\min})$.

Convergence is achieved after 18 iterations (Fig.6a). The optimized geometry in Fig. 5b exhibits smooth global modifications enabled by the ring-based smoothing. While the overall broadband SPL reduction is modest (≈ 1 dB), localized improvements are observed at specific microphone locations (Fig.6b). To highlight the computational gains using the IGABEM MOR framework, the traditional FOM approach would require $18 \times 12 \times 1000 = 216,000$ full system evaluations, making design optimization with FOMs inefficient (see Table 3). In contrast, the IGABEM MOR framework enables rapid design optimization by evaluating a much smaller amount of full system evaluations, accelerating the broadband design iterations.

Table 1: Off-line cost of the two-step MOR.

Operation	Time
Construction of $\mathbf{W}$ and $\mathbf{V}_{\mathrm{RBM}}$	17 min
Construction of $\mathbf{T}_i$	39 min
Total off-line cost	56 min

Table 2: On-line cost for 1000 frequency evaluations.

	FOM	ROM	Speed-up
Assembly	26 h 7 min	29 s	3.2×10^3
Solution	1 min	0.4 s	150

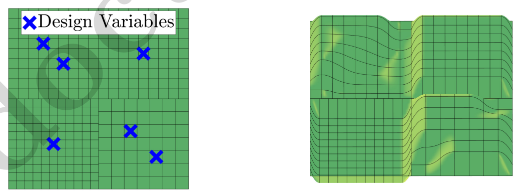

(a) Initial flat plate geometry with 6 design variables **(b)** Optimized flat plate geometry

Figure 5: Design variables and optimized geometry.

6. Conclusion

In this work, an efficient IGABEM MOR framework is introduced for acoustic frequency sweep analyses and broadband design iterations. The framework employs a non-intrusive two-step MOR utilizing Chebyshev polynomials, Krylov-subspace recycling and RBM to reduce computational costs while preserving accuracy. The performance of the method was demonstrated on an academic test case, a flat plate subjected to a monopole source, where substantial speed-ups were achieved for broadband acoustic simulations. The ROMs enabled computationally feasible shape optimization over a wide frequency range which would be impractical using the FOM. By performing geometry updates directly at the control point level and incorporating a ring-based smoothing strategy, the framework maintains CAD consistency and prevents unrealistic localized deformations that may arise in finely discretized high-frequency IGA models, thus allowing robust design iterations without remeshing. The proposed framework provides therefore a computationally efficient and fully CAD-based workflow for broadband acoustic design exploration.

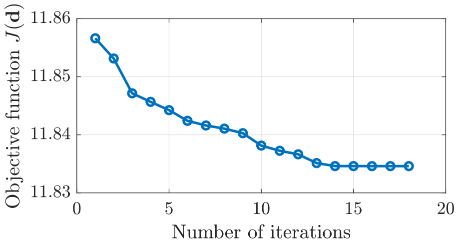

(a) Convergence plot for broadband shape optimization

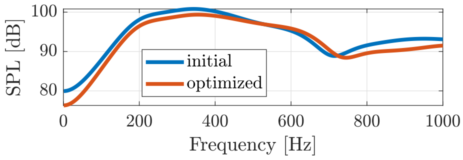

(b) SPL spectrum at $(0.65, 0.65, -0.5)$ m

Figure 6: Convergence plot and SPL reduction

Table 3: Optimization summary multi-patch flat plate problem.

Design variables	6
Convergence iteration	18
Number of particles	12
Frequency range	1-1000 Hz
Total full size system evaluations (FOM)	216,000
Total full size system evaluations (ROM)	7,344

7. Acknowledgments

The research of P. Le is funded by "Design for IGA-type discretization workflows (GECKO)" project which receives funding from the European Union's Horizon Europe research and Innovation programme under grant agreement No 101073106 Call: HORIZON-MSCA-2021-DN-01. Views and opinions expressed are however those of the authors only and do not necessarily reflect those of the European Union. The European Union cannot be held responsible for them.

References

[1] P. Le, D. Panagiotopoulos, and E. Deckers, "A non-intrusive efficient two-step model reduction method for large-scale thin-walled acoustic indirect bem systems," *International Journal for Numerical Methods in Engineering*, vol. 126, no. 20, e70171, 2025.

[2] C. A. Brebbia, "The boundary element method for engineers," 1978.

[3] T. Hughes, J. Cottrell, and Y. Bazilevs, "Isogeometric analysis: Cad, finite elements, nurbs, exact geometry and mesh refinement," *Computer Methods in Applied Mechanics and Engineering*, vol. 194, no. 39, pp. 4135–4195, 2005, ISSN: 0045-7825.

[4] R. Simpson, M. Scott, M. Taus, D. Thomas, and H. Lian, "Acoustic isogeometric boundary element analysis," *Computer Methods in Applied Mechanics and Engineering*, vol. 269, pp. 265–290, 2014, ISSN: 0045-7825.

[5] L. Coox, O. Atak, D. Vandepitte, and W. Desmet, "An isogeometric indirect boundary element method for solving acoustic problems in open-boundary domains," *Computer Methods in Applied Mechanics and Engineering*, vol. 316, pp. 186–208, 2017, Special Issue on Isogeometric Analysis: Progress and Challenges, ISSN: 0045-7825.

[6] G. C. Diwan and M. S. Mohamed, "Pollution studies for high order isogeometric analysis and finite element for acoustic problems," *Computer Methods in Applied Mechanics and Engineering*, vol. 350, pp. 701–718, 2019.

[7] D. Panagiotopoulos, E. Deckers, and W. Desmet, "A two-step reduction method for acoustic BEM systems," in *Forum Acusticum*, Lyon, France, Dec. 2020, pp. 2291–2298.

[8] D. Panagiotopoulos, W. Desmet, and E. Deckers, "An automatic krylov subspaces recycling technique for the construction of a global solution basis of non-affine parametric linear systems," *Computer Methods in Applied Mechanics and Engineering*, vol. 373, p. 113 510, 2021, ISSN: 0045-7825.

[9] P. Le, D. Panagiotopoulos, E. O. Inci, and E. Deckers, "Model order reduction towards efficient shape optimization for non-conforming multi-patch isogeometric boundary element method," Manuscript submitted for publication, 2026.

[10] P. Filippi, "Layer potentials and acoustic diffraction," *Journal of Sound and Vibration*, vol. 54, no. 4, pp. 473–500, 1977.

[11] T. Liang, J. Wang, J. Xiao, and L. Wen, "Coupled be–fe based vibroacoustic modal analysis and frequency sweep using a generalized resolvent sampling method," *Computer Methods in Applied Mechanics and Engineering*, vol. 345, pp. 518–538, 2019.

[12] W. E. Arnoldi, "The principle of minimized iterations in the solution of the matrix eigenvalue problem," *Quarterly of Applied Mathematics*, vol. 9, no. 1, pp. 17–29, 1951, ISSN: 0033569X, 15524485. Accessed: May 4, 2024.

[13] Å. Björck, "Numerics of gram-schmidt orthogonalization," *Linear Algebra and its Applications*, vol. 197-198, pp. 297–316, 1994, ISSN: 0024-3795.

[14] S. K. Baydoun, M. Voigt, C. Jelich, and S. Marburg, "A greedy reduced basis scheme for multifrequency solution of structural acoustic systems," *International Journal for Numerical Methods in Engineering*, vol. 121, no. 2, pp. 187–200, 2020.